Localized Dynamic Light Scattering: Probing Single Particle Dynamics at the Nanoscale

R. Bar-Ziv,[1] A. Meller,[1] T. Tlusty,[2] E. Moses,[1] J. Stavans,[1] and S. A. Safran[2]
[1]*Department of Physics of Complex Systems, The Weizmann Institute of Science, Rehovot 76100, Israel*
[2]*Department of Materials and Interfaces, The Weizmann Institute of Science, Rehovot 76100, Israel*
(Received 28 August 1996)

We developed an experimental technique which probes the dynamics of a single colloidal particle over many decades in time, with spatial resolution of a few nanometers. By scattering a focused laser beam from a particle observed in an optical microscope, we measure its fluctuations via the temporal autocorrelation function of the scattered intensity $g(t)$. This technique is demonstrated by applying it to a single Brownian particle in an optical trap of force constant k. The decay times of $g(t)$, which are related to the particle position autocorrelation function, scale as k^{-1}, as expected from theory. [S0031-9007(96)02028-5]

PACS numbers: 87.64.–t, 05.40.+j, 42.25.Fx

Dynamic light scattering (DLS) has become a powerful technique for measuring dynamics of colloidal particles over many decades in time down to the nanosecond regime [1]. In a typical DLS experiment a laser beam impinges on a sample volume which contains a large number of scatterers. The scattered light collected by a detector far from the sample is generated by the interference of light scattered from all the particles. The random thermal motion of these particles shifts the relative phases of the scattered fields and yields temporal intensity fluctuations. In such experiments, where the beam waist varies over scales which are much larger than the particles and their motion, a *single* isolated particle will scatter light with constant intensity and hence will not produce temporal intensity correlation.

However, in many cases the dynamics of an isolated, possibly complex, object is of interest. This situation is common in the biological realm where objects such as cells, organelles, or even protein macromolecules have a rich dynamics that depends on their structure and local environment. Examples range from motor proteins moving along polymeric fibers [2] to the elastic flickering of red blood cell membranes [3]. Direct access to the dynamics of localized single entities thus would allow for scrutiny of complex biological processes at high resolution.

In this paper, we present a new technique called localized dynamic light scattering (LDLS). It incorporates both DLS and optical microscopy in a direct measurement of the position autocorrelation function of a single object. While DLS has been implemented with optical microscopy in previous works [4], the present work extends DLS to probe the dynamics of a single particle. This is achieved by illuminating the object with a strongly focused laser beam whose intensity profile changes over scales comparable to the size of the object. The autocorrelation function (ACF) is therefore based on intensity fluctuations due to the single particle and not on phase interference from many particles nor on number fluctuations [5]. The scattered light is collected using an optical fiber probe that can be placed and manipulated in close proximity to the particle. The light is transferred via the fiber to a photodetector whose signal is fed to a digital correlator where the temporal intensity autocorrelation function, which contains information on the particle dynamics, is computed. The scattering object can be either a rigid particle, such as a glass bead, or a particle with internal degrees of freedom, such as a cell membrane or any other organelle. We present the physical principles of this technique and describe a simple experiment where a single spherical particle is held in a potential well that is formed with optical tweezers [6].

In a LDLS experiment the scattering volume is of the order of $\sim\lambda^3$, where λ is the wavelength of the scattering light source. This is achieved by illuminating the sample through a microscope objective lens producing a sharply peaked intensity profile near the focus. Assuming an incident cylindrical symmetric beam propagating along the z axis we approximate the intensity profile by a Gaussian [7] $I_{\rm inc} \sim \prod_i \exp[-r_i^2/2(\omega_i^S)^2]$, where ω_i^s is the waist of the axially symmetric ($\omega_x^S = \omega_y^S$) beam and $i = x, y, z$. This allows scattering from only a well defined region in the sample given by beam waists that are of the order of λ. Within this region we consider a single pointlike scatterer whose position relative to the beam focus is $\vec{r}(t)$. In this case the scattered intensity I_s changes in time only due to the motion inside the inhomogeneous beam, and hence $I_s(t) \sim I_{\rm inc}(\vec{r}(t))$. The intensity ACF is therefore

$$g(t) = \langle I_s(0) I_s(t) \rangle \sim \left\langle \prod_i \exp\left[-\frac{r_i^2(0) + r_i^2(t)}{2(\omega_i^S)^2} \right] \right\rangle . \quad (1)$$

Note that $g(t)$ depends on time only through $r_i(t)$. We have demonstrated that the LDLS technique works by applying it to a Brownian particle inside a potential well. We first describe the experiment and then calculate $g(t)$ from a dynamical model for the particle motion.

Figure 1 is a sketch of the experimental setup. A spherical silica bead suspended in water was trapped by a strongly focused laser beam with a spot of dimensions ω_i^T

 0031-9007/96/78(1)/154(4)$10.00

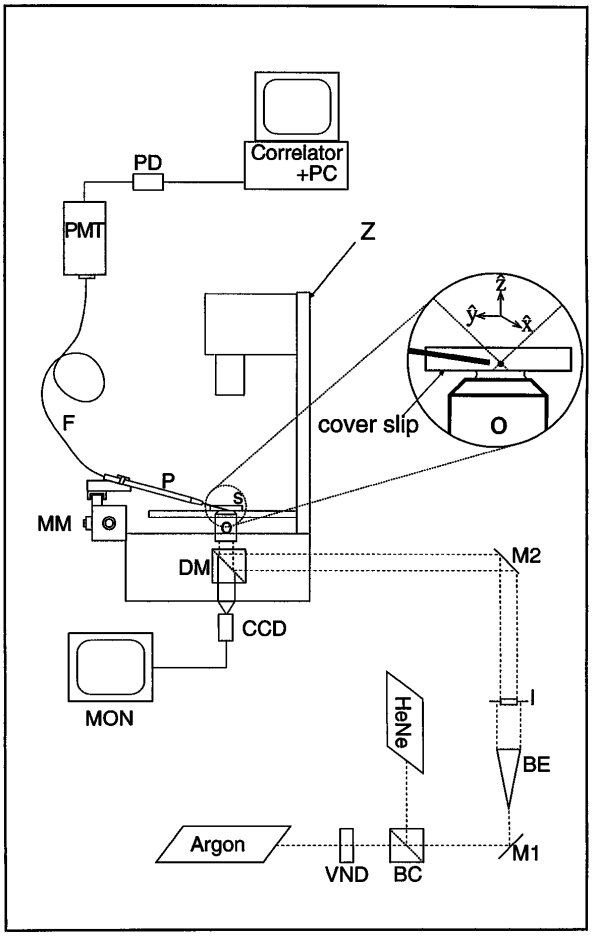

FIG. 1. Schematic drawing of the LDLS setup. Argon: argon laser (Coherent Innova 70) operating in the 514.5 line, coupled via a single mode fiber. VND: variable neutral density filter. HeNe: HeNe laser (Uniphase 1125P). BC: beam cube, M1 and M2: mirrors. BE: beam expander composed of two positive lenses, I: Iris diaphragm. Z: inverted microscope (Zeiss Axiovert 135). DM: dichroic mirror. CCD: charge-coupled device camera. MON: monitor and video recorder. O: microscope objective (Zeiss plan-apochromat x63/1.4. S: sample. P: pipette holder used to support the fiber detector. MM: micromanipulator (Narashige MHW-13). F: single mode fiber with 4 μm core diameter. PMT: photomultiplier tube with 628.3 nm line filter (Thorn EMI 9863B/100). PD: preamplifier and discriminator (Thorn EMI), Correlator: digital correlator (Brookhaven instruments BI-9000). Inset: close-up view of the scattering cell.

and tunable intensity I_0^T. The optical tweezers were set up using an inverted microscope, a high numerical aperture lens, and a (514.5 nm) green argon laser. The bead of radius 0.5 μm was trapped about 50 μm above the bottom cover slip (see inset of Fig. 1). To control independently the trap force and the scattering intensity, we used a red (632.8 nm) HeNe laser, collinear with the green laser, as the scattering light source. The relative intensities of the two lasers was less than 1/100, and hence the trapping effect of the weaker red laser could be neglected. The fiber probe was positioned about 100 μm away from the optical axis forming an angle of 75° with the incident direction. A 632.8 nm line filter in front of our detector ensured that only the red light was actually probed. Fine adjustments of the probe (enabled by a sensitive micromanipulator) were carried out in order to optimize the signal to noise ratio. For any given trapping intensity I_0^T, a few minutes were sufficient to acquire a smooth correlation function.

The resulting potential well that is formed by the green laser is approximately harmonic [8], with a restoring force $-k_i r_i$ acting on the particle. The spring constant k_i is directly proportional to the trap intensity I_0^T, to the polarizability of the particle α, and inversely proportional to the square of the trap width, $k_i = I_0^T \alpha/(\omega_i^T)^2$. If the restoring force is strong enough it confines the particle within the trap, and hence its motion has an exponentially decaying position ACF [9]:

$$\langle r_i(0) r_i(t)\rangle = \bar{r}_i^2 \exp(-t/\tau_i)\,, \tag{2}$$

with $\tau_i = 6\pi R\eta/k_i$. R is the radius of the particle and η is the viscosity of the surrounding solution [10]. The mean square fluctuation of the particle is $\bar{r}_i^2 = k_B T/k_i$, where T is the temperature and k_B is the Boltzmann constant.

Since both the scattered and the trapping laser are collinear and focused through the same lens, the intensity ACF, Eq. (1), becomes a product of three decoupled Gaussians: $g(t) \sim \prod_i \langle \exp[-\frac{r_i^2(0)+r_i^2(t)}{2(\omega_i^S)^2}]\rangle$. In order to proceed further we perform the averages using both the particle position distribution function $P(r_i) \sim \exp(-r_i^2/2\bar{r}_i^2)$ [9] and the position correlation function, Eq. (2). The resulting normalized intensity ACF is [11]

$$\tilde{g}(t) = \frac{\langle I_s(0) I_s(t)\rangle}{\langle I_s(0)\rangle^2} = \prod_i \frac{1}{\sqrt{1 - S_i \exp(-2t/\tau_i)}}\,, \tag{3}$$

where $0 \le S_i \le 1$ is a dimensionless parameter which takes into account the ratio of the scattering beamwidth and the mean square fluctuations in the well, $S_i = [1 + (\omega_i^S)^2/\bar{r}_i^2]^{-2}$.

In the case of a strong trap, where the mean square fluctuations are smaller than the scattering laser waists $\bar{r}_i^2 \ll (\omega_i^S)^2$, an expansion of Eq. (3) yields a sum of three decoupled exponential functions,

$$\begin{aligned}\tilde{g}(t) &\simeq 1 + \frac{1}{2}\sum_i S_i \exp\left(\frac{-2t}{\tau_i}\right) \\ &\simeq 1 + \frac{1}{2}\sum_i \left(\frac{T}{k_i(\omega_i^S)^2}\right)^2 \exp\left(\frac{-2t}{\tau_i}\right),\end{aligned} \tag{4}$$

which may be reduced to two independent exponential functions due to the axial symmetry in our system. In the case of a weak trap where the mean square fluctuations are much larger than the beam waists, $\bar{r}_i^2 \gg (\omega_i^S)^2$, the particle randomizes its motion before acquiring potential energy. Therefore it exhibits random diffusive motion for

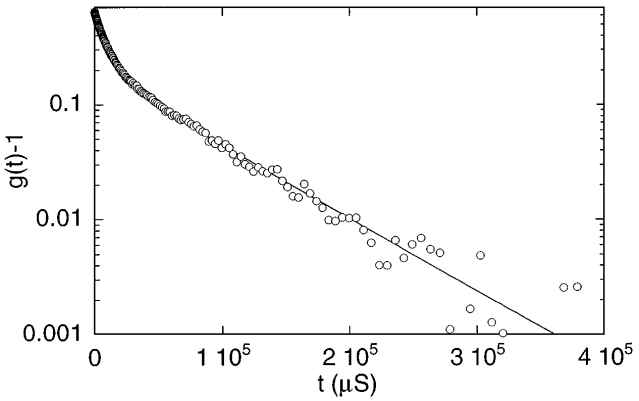

FIG. 2. Typical normalized intensity autocorrelation function measured for a silica bead of radius 0.5 μm. The semilog plot manifests the two decay times resulting from the different trapping widths in the axial and transverse directions. The solid line is a fit using Eq. (3).

short times, $t \ll \tau_i$, and then Eq. (3) predicts a power law $g(t) \sim t^{-3/2}$ which we have not yet measured.

A typical ACF is shown in Fig. 2 together with a fit using Eq. (3). We readily identify two well separated decay times, in accordance with Eq. (4). Figure 3 shows a plot of the two time scales obtained from the fits as a function of laser intensity. Both plots yield an inverse power law $\tau_i \sim 1/I_0^T$ as expected from the theory. The longer time scale corresponds to motion in the longitudinal direction while the shorter time scale is related to the transverse motion. Using the relation $\tau = 6\pi R\eta/k$, we obtain the values of the force constants k as a function of laser intensity I_0^T for both time scales. In the inset of Fig. 3 we plot $1/\tau$ as a function of k for both the longitudinal and the transverse directions, and obtain data collapse onto one curve. The shortest mean square displacement here

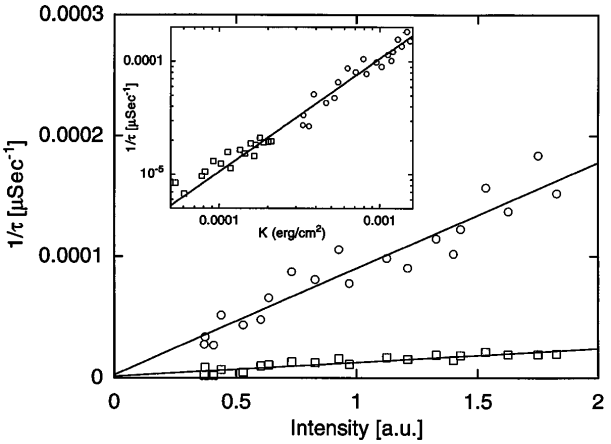

FIG. 3. Plot of the inverse time scales for the axial (squares) and transverse (circles) motion of the particle in the three-dimensional potential well versus the laser intensity. Inset: collapse of the two time scales when replotted as functions of force constant k, obtained from the intensity using the theoretical relation $\tau_i = 6\pi R\eta/k_i$ (see text).

is ~10 nm, corresponding to the shortest time measured, but our technique allows much better resolution in time and thus better spatial resolution if, for example, smaller particles are used. We note that we can extract the anisotropy of the optical trap from the measured decay times $\omega_x^T/\omega_z^T = \sqrt{\tau_x/\tau_z} = 0.4$.

The above ACF, Eq. (3), is exact only for a point-like particle which scatters isotropically. However, for a spherical particle which does not scatter isotropically, the temporal behavior of the ACF is not altered as long as the particle executes small excursions compared with the scattering beam waist [11,12]. In our experiment the mean square amplitude of the particle in the optical trap is at most of the order of the trap size. Therefore the use of Eq. (3) to analyze the measured ACF is justified. We note that the high signal to noise ratio obtained is a result of both our light collection geometry and its positioning in the vicinity of a scattering minimum. A simple calculation that substantiates this experimental observation will be published elsewhere [11].

We have presented the salient features of the new LDLS technique and described an experiment with a single particle trapped in a potential well. The scattering of an inhomogeneous beam from a localized particle provides direct information on the three-dimensional motion of the particle. DLS from single particles under a microscope may have diverse applications in biophysics. Scattering from more complex structures such as cell membranes and organelles can provide dynamical information down to the nanoscale.

We acknowledge useful discussions with E. Bar-Ziv, Y. Barad, P. Chaikin, H. Davidowitz, E. Domany, M. Elbaum, A. Groisman, T. Mason, B. Menes, O. Krichevsky, V. Steinberg, Y. Silberberg, D. Weitz, and M. Wong. We thank V. Frette for a critical reading of the manuscript. A. M. acknowledges support from the Israeli Ministry of Science and Arts. This work was supported in part by the Israeli Ministry of Science and Arts Grant No. 5879 , the Minerva Foundation, Munich, and the Minerva Center for Nonlinear Science.

[1] B. J. Berne and R. Pecora, *Dynamic Light Scattering: With Applications to Chemistry, Biology and Physics* (Wiley, New York, 1976); *Dynamic Light Scattering, The Method and some Applications*, edited by Wyn Brown (Clarendon Press, Oxford, 1993).

[2] S. C. Kuo and M. Sheetz, Science **260**, 232 (1993); K. Svoboda, C. F. Schmidt, D. Branton, B. J. Schnapp, and S. M. Block, Nature (London) **365**, 721 (1993); J. T. Finer, R. M. Simmons, and J. A. Spudich, Nature (London) **368**, 113 (1994); K. Svoboda, P. P. Mitra, and S. M. Block, Proc. Natl. Acad. Sci. U.S.A. **91**, 11 782 (1994); H. Yin, M. D. Wang, K. Svoboda, R. Landick, S. M. Block, and J. Gelles, Science **270**, 1653 (1995).

[3] F. Brochard and J. F. Lennon, J. Phys. (Paris) **36**, 1035 (1975); H. Strey, M. Peterson, and E. Sackmann, Biophys. J. **69**, 478 (1995).
[4] See, for example, Z. Kam and R. Rigler, Biophys. J. **39**, 7 (1982); K. Schatzel, W. G. Neumann, J. Muller, and B. Materzok, Appl. Opt. **31**, 770 (1992).
[5] See, for example, D. W. Schaefer and B. J. Berne, Phys. Rev. Lett. **28**, 475 (1972); D. Magde, E. Elson, and W. W. Webb, Phys. Rev. Lett. **29**, 705 (1972).
[6] A. Ashkin, Phys. Rev. Lett. **24**, 156 (1970); Science **210**, 1081 (1980); A. Ashkin, J. M. Dziedzic, and T. Yamane, Nature (London) **330**, 769 (1987).
[7] A. Yariv, *Optical Electronics* (HRW Saunders College Pub., Chicago, 1991).
[8] K. Svoboda and S. M. Block, Annu. Rev. Biophys. Biomol. Struct. **23**, 247 (1994); R. M. Simmons, J. T. Finer, S. Chu, and J. A. Spudich, Biophys. J. **70**, 1813 (1996).
[9] P. M. Chaikin and T. C. Lubensky, *Principles of Condensed Matter Physics* (Cambridge University Press, Cambridge, England, 1995); M. Doi and S. F. Edwards, *The Theory of Polymer Dynamics* (Clarendon Press, Oxford, 1988).
[10] We neglect the inertial of the particle that would give rise to a fast time scale $\tau = m/\zeta$ (shorter than 1 μsec for μm size silica particles).
[11] A. Meller *et al.* (to be published).
[12] This is because the primary contribution of both the point particle and the finite sized particle scale as $\langle r_i^2(0) r_i^2(t) \rangle$.